Annual variation in baroclinic structure of the northwestern tropical Pacific

Gary MEYERS (1), Warren WHITE (1),
and Keiichi HASUNUMA (2)

ABSTRACT

Annual variation in temperature of the upper 400 m of the northwestern tropical Pacific is studied on the basis of 45,000 observations taken with MBTs, XBTs, and hydrographic casts. The original data are reduced to monthly averages on a 2.5 ° latitude by 5 ° longitude grid at standard depths. The mean annual variation is decomposed into annual and semiannual components by harmonic analysis. In the subtropical region north of 20 °N, the largest annual variations occur in the upper 100 m. Annual phase increases with depth suggesting an obvious connection to variation in heat flux through the sea surface. In the tropics south of 15 °N, the largest temperature variations occur within the depth range of the main thermocline. There, annual and semiannual phase are constant in the depth range of the main thermocline, consistent with a baroclinic response to atmospheric forcing. Dynamic height 0|200 db calculated from the vertical temperature integral is dominated by the surface thermohaline regime north of 20 °N and the subsurface baroclinic response south of 15 °N. Both processes play a role in the annual variation in strength of currents of the subtropics. Interannual, annual, and semiannual variability are compared, showing that all three have high variance in the region between the equator and 10 °N. This suggests the hypothesis that modulation or interruption of the atmospheric processes maintaining the annual or semiannual variation may play a role in forcing the interannual variation.

KEY WORDS : Temperature — Surface — Subsurface Currents — Variability.

RÉSUMÉ

VARIATION ANNUELLE DE LA COUCHE BAROCLINE DANS LE PACIFIQUE TROPICAL NORD OCCIDENTAL

La variation annuelle de la température dans les 400 premiers mètres du Pacifique tropical nord-occidental est étudiée à partir de 45 000 observations provenant de BT, XBT et stations hydrologiques. Les données originales sont ramenées à des moyennes mensuelles, calculées par maille de 2,5° de latitude par 5° de longitude, aux profondeurs standard. La variation annuelle moyenne est décomposée en ses termes annuel et semi-annuel par une analyse harmonique. Dans la région subtropicale, au nord de 20° N, les plus fortes variations annuelles ont lieu dans les 100 premiers mètres. La phase de la composante annuelle croît avec la profondeur, suggérant une relation avec la variation du flux de chaleur à travers la surface de la mer. Sous les tropiques, au sud de 15° N, les variations les plus élevées de la température sont observées à l'intérieur de la gamme de profondeur de la thermocline principale; dans cette zone, les phases de composantes annuelle et semi-annuelle sont constantes au sein de la couche ou l'on rencontre la thermocline, ce qui est cohérent avec une réponse barocline au phénomène d'entraînement atmosphérique. La hauteur dynamique 0|200 db, calculée à partir de l'intégrale verticale du profil de température, est dominée par le

(1) *Scripps Institution of Oceanography University of California, San Diego, U.S.A.*
(2) *Ocean Research Institute University of Tokyo, Japan.*

régime thermohalin de surface au nord de 20° N et par la réponse barocline de subsurface au sud de 15° N. Les deux mécanismes jouent un rôle dans la variation annuelle d'intensité des courants de la zone subtropicale. Les variabilités inter-annuelle, annuelle et semi-annuelle sont comparées et il est montré que la variabilité semi-annuelle et la variabilité inter-annuelle sont caractérisées par de fortes variances dans la zone comprise entre l'Équateur et 10° N. Cela induirait l'hypothèse selon laquelle la modulation ou l'interruption des phénomènes atmosphériques, responsables de la variation semi-annuelle, pourraient influer, en l'accentuant, sur la variation inter-annuelle.

MOTS-CLÉS : Température — Surface — Subsurface — Courants — Variabilité.

1. INTRODUCTION

The strength of the equatorial current system in the western tropical Pacific Ocean is associated with annual variation in atmospheric forcing. The strength of the North Equatorial Current and Countercurrent have nearly the same phase reaching a maximum during late fall and winter (WYRTKI, 1974a). The Subtropical Countercurrent near 20° N reaches maximum strength a few months later during spring UDA and HASUNUMA, 1969; WHITE *et al.*, 1978).

These annual cycles have been related to atmospheric forcing in several studies. The North Equatorial Countercurrent is strongest when the easterly wind blowing against it is weak and the Intertropical Convergence Zone (ITCZ) is located directly over it. The current is weakest when the ITCZ shifts southward, permitting the full strength of the northeast trades to blow against it (WYRTKI, 1974b). A simple adiabatic model of the baroclinic structure of this annual cycle in the eastern and central Pacific was tested by MEYERS (1975, 1979). The model permits a local response in the main thermocline to the vertical Ekman pumping velocity (divergence of Ekman transports calculated from wind stress) and a remote response due to non-dispersive Rossby waves radiating from the regions of most intense forcing. The model indicates that the main thermocline is largely pumped by the local wind stress north of the Countercurrent, while a Rossby wave is generated south of the Countercurrent.

The simple dynamical model connecting the response in the equatorial current system to forcing by the trade winds reveals deficiencies when compared in detail to observations (MEYERS, 1979). This suggests that some important dynamics are missing from the model. The deficiencies also suggest that the observational data base may be inadequate in some areas. Further progress in these studies will only be made by improving the observational data base.

A descriptive study of the mean annual baroclinic response in the western tropical Pacific is needed at this time because several numerical models of the tropical ocean, forced by an annually varying atmosphere, have been developed recently (HANEY *et al.*, 1978; LEROY, 1979; HUANG, 1979; COX, 1980; BUSALACCI and O'BRIEN, 1980). A description of the observed oceanic response, with some indication of the possible errors in the analysis, is needed for comparison to these models. Also, a new X.B.T. observational program taking monthly to fortnightly temperature sections between New Caledonia and Japan recently began in the region (MEYERS and DONGUY, 1980). Comparison of the new temperature observations to the climatological annual cycle representative of the past three decades will be useful at the outset.

2. DATA SOURCES AND DATA PROCESSING

The temperature data used in this study were taken from the archives of the National Oceanographic Data Center (N.O.D.C.), Washington, D.C., and the Japanese Far Seas Fisheries (J.F.S.F.) Service, Shimizu, Japan. Approximately 45,000 stations were available after combining the oceanographic station data, the expendable bathythermographic (X.B.T.) data, and the mechanical bathythermographic (M.B.T.) data. The N.O.D.C. data cover the period 1954-1976. The J.F.S.F. data are exclusively M.B.T.'s. They cover the period 1967-1971, and are concentrated principally in the region from the equator to 25° N, where the N.O.D.C. data are sparse. They comprise more than 60 % of the data taken in the western tropical Pacific during these years. Further details on the data sources are given in WHITE and WYLIE (1977).

Longterm monthly mean fields of temperature on a 2.5° latitude by 5° longitude grid were computed at standard depths (0, 10, 20, 30, 50, 75, 100, 150, 200, 300, 400 m). Individual temperature observations which deviated from the mean by more than 3 standard deviations were rejected as questionable data. The geographic distribution of the remaining data at the 100 m level is given in figure 1, which also shows the region of interest in this study.

WYRTKI (1974a) has shown that sea level is a good index of dynamic height or subsurface temperature in this region. Spectral analysis of sea level at islands shows prominent peaks at the

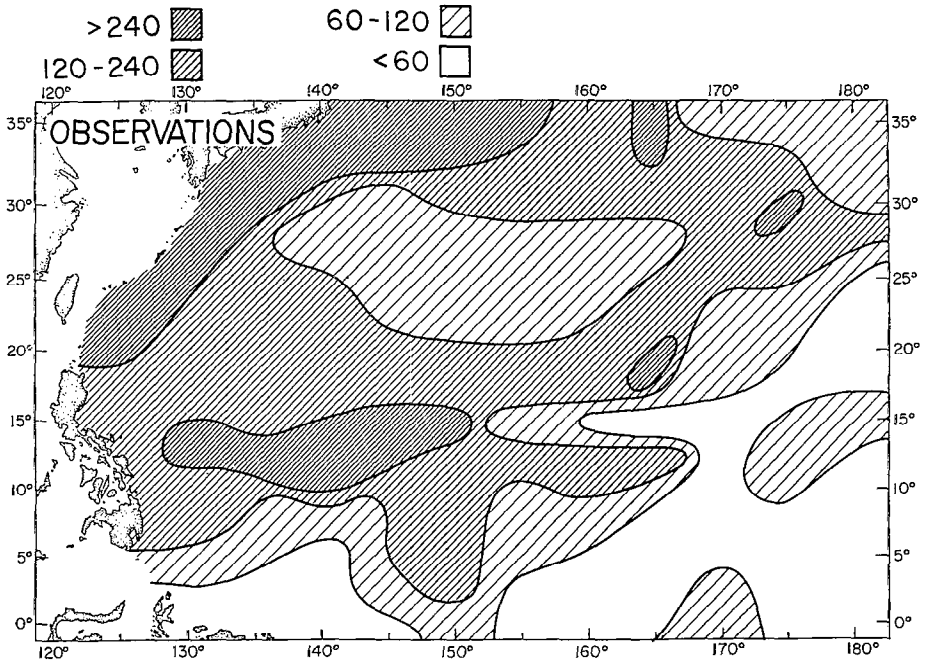

Fig. 1. — Number of subsurface temperature observations per 2.5°-latitude by 5°-longitude quadrangle.
Nombre d'observations de la température dans la couche 0-400 m, par maille de 2,5° en latitude et 5° en longitude.

annual and semiannual frequencies (WYRTKI, 1974b, p. 377) superimposed on a background variability which increases in energy density toward lower frequency (i.e. a red background). The existence of the annual component is not surprising because of the strong seasonal atmospheric forcing everywhere on the ocean. The semiannual component is not as well known; however its amplitude exceeds the annual amplitude at several islands in the western Pacific between the equator and 10° N (WYRTKI and LESLIE, 1980, p. 29). The existence of these peaks in sea level spectra suggests that the monthly mean temperature data can be interpreted as annual and semiannual components.

The amplitude (A_i) and phase ($\varnothing_i$) of annual (i=1) and semiannual (i=2) variation was estimated by fitting the mean temperature values by the method of least squares with a model of the form :

$$T(t)=T+\sum_{i=1}^{2} A_i \cos(\mu_i t-\varnothing_i)$$

In this model the longterm annual mean temperature is T, time since 1 January is t, and frequency is μ_i. Regions that had less than 10 monthly mean values, or that had two consecutive missing values, were eliminated. The regions with adequate data are enclosed on the maps with a dashed line. Harmonic analysis gives identically the same result as the method of least squares at grid points with 12 values. The percentage of grid points with 12, 11, or 10 values was respectively 67 %, 19 %, and 14 %.

In order to interpret maps of the amplitude and phase (presented later), it is necessary to know how precise the estimates are. The standard deviation of amplitude and phase can be determined from the annual RMS deviation of monthly mean temperatures (σ) and the estimated amplitudes. The RMS residual variance (δ^2) after specification of the annual (A_1) and semiannual (A_2) amplitude is

$$\delta^2=\sigma^2-\sum_{i=1}^{2} 1/2\ A_i^2$$

The error in phase is then δ/A, which is approximately equal to twice the standard deviation in phase (BLOOMFIELD, 1976, p. 28). The error in amplitude is δ and is also approximately equal to twice the standard deviation in amplitude. Maps of σ accompany maps of A_i and $\varnothing_i$ so that amplitude and phase errors can be estimated for any location. Error estimates for one example are given in section 5.

Horizontal maps of the amplitude and phase show that major features are aligned nearly east-west, except near the western boundary. Averages

were, therefore, computed again using a larger longitudinal area (142.5° E-157.5° E), and the harmonic analysis was repeated. In this case grid points with less than 11 values were eliminated.

The accuracy of the longterm mean monthly temperatures depends on instrumental error, subgrid variability, and interannual variability, the last being the most energetic source of error (MASUZAWA and NAGASAKA, 1975). Standard deviation of interannual variability (fig. 2) was obtained by averaging the variance of the 12 monthly means at each grid point. The largest interannual variance is located in the tropical thermocline near 150 m and in the deeper thermocline near 35° N beneath the Kuroshio. Variance beneath the Kuroshio may also be associated with eddy-scale phenomena (BERNSTEIN and WHITE, 1977; WILSON and DUGAN, 1978).

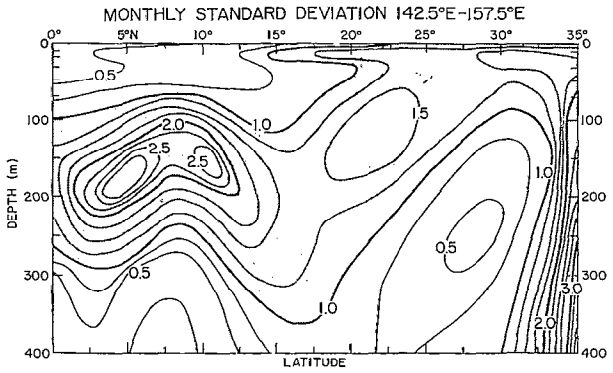

Fig. 2. — Typical values of standard deviation in monthly mean temperature, averaged in 2.5°-latitude by 15°-longitude quadrangles in the zone 142.5°E to 157.5°E. Typical values were estimated by averaging 12 monthly values of temperature variance.

Écart-type à la moyenne mensuelle des températures, par rectangle de 2,5° en latitude et 15° en longitude, de la zone allant de 142,5° E à 157,5° E; ces valeurs sont calculées en faisant la moyenne des variances mensuelles de la température.

The mean annual cycle in this study was computed from a composite of data from all years. The interannual variability in the region south of 15° N may have a significant effect on the computed mean annual cycle because the largest interannual anomalies tend to occur at a preferred time of year (RASMUSSON and CARPENTER, 1980). Neither the magnitude of this effect nor the spatial extent of the region where it is significant is known. Because of this effect it is possible that some features of the computed annual cycle in this study may be intermittent phenomena, present during some years and not during others, rather than a stationary cycle.

3. HORIZONTAL TEMPERATURE FIELD

The horizontal distribution of annual variation in temperature, and its relationship to the mean field are discussed in this section. The results for the surface are consistent with a similar analysis by WYRTKI (1965), based on ship injection temperatures. The surface variability is contrasted with variability at 100 m within the thermocline.

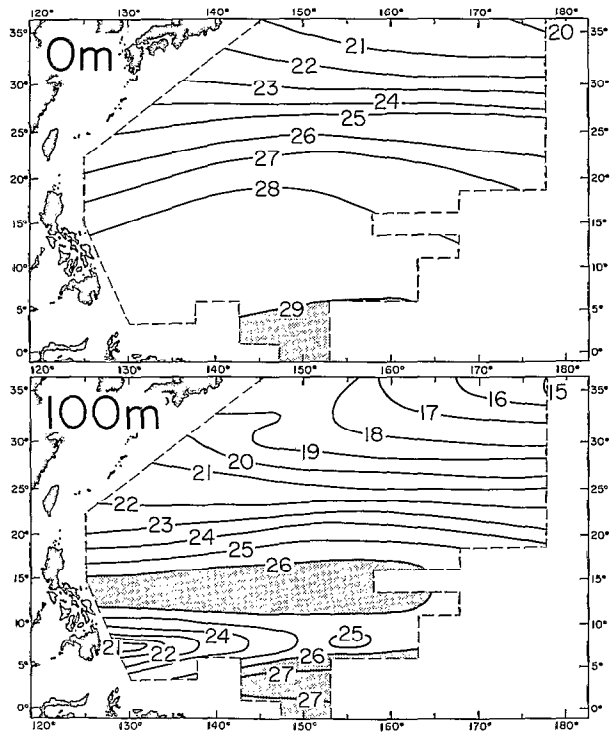

Fig. 3. — Annual longterm mean temperature.

Température annuelle moyenne sur une longue période.

The long term mean temperature at 0 m and 100 m is shown in fig. 3. Temperature at 100 m is characterized by a series of ridges and troughs which are well known from standard references (ROBINSON and BAUER, 1976; JODC, 1975; U.S.S.R. Navy, 1976). These features were recently discussed by WHITE and HASUNUMA (1980), who defined names for them which are used below.

The annual RMS deviation calculated from the longterm monthly mean temperatures (fig. 4) shows a vertical contrast with large surface variance in the subtropics north of 20° N and large subsurface variance in the tropics, south of 15° N. Apparently at least two distinct processes influence the temperature field, an obviously diabatic (heating and cooling) process in the subtropical surface water; and another process in the tropical thermocline.

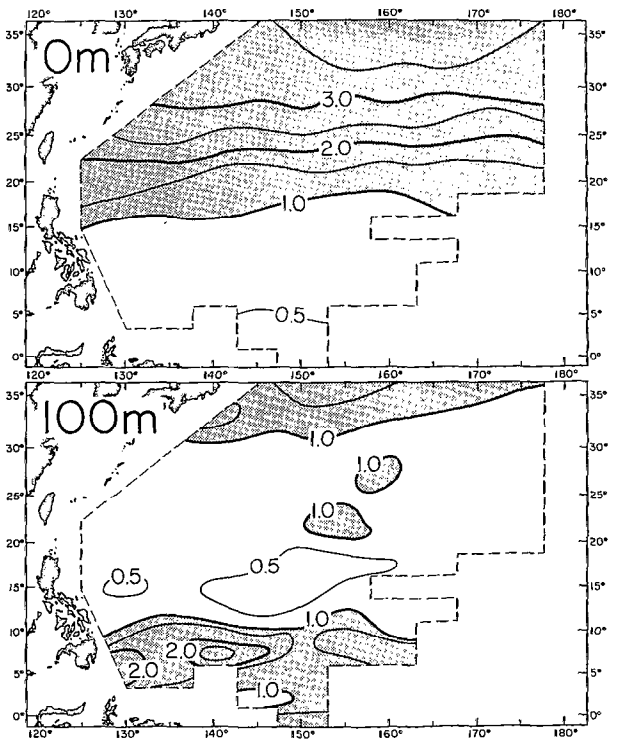

Fig. 4. — RMS deviation of monthly mean temperatures.
Écart quadratique moyen de la température mensuelle moyenne.

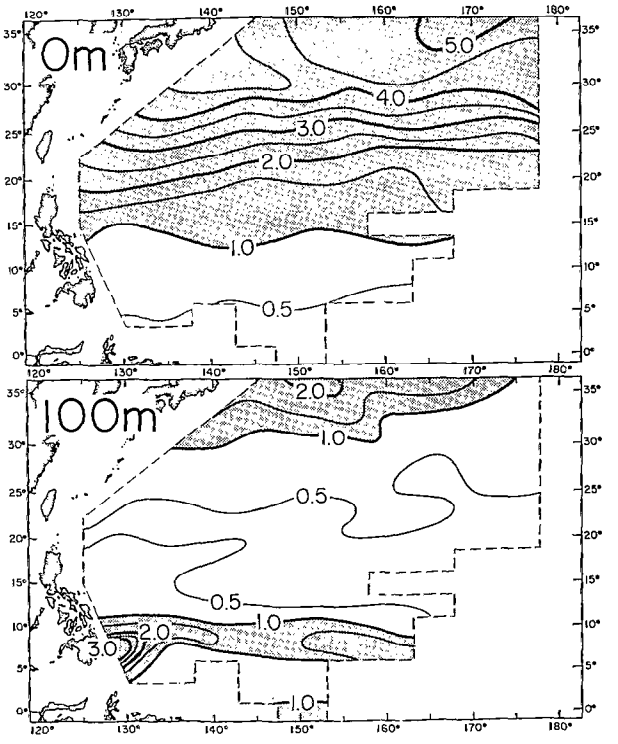

Fig. 5. — Annual amplitude of temperature variation.
Amplitude annuelle de la variation de température.

The annual (1 cpy) amplitude also shows this vertical contrast (fig. 5). The frequency decomposition shows that the subsurface variations are aligned along bands corresponding to the ridges and troughs in the main thermocline. In contrast, the surface amplitude and phase have a much larger meridional space scale, which transcends the mean baroclinic structure. This indicates a de-coupling of the annual cycle of surface temperature from that of the thermocline. Note that temperature in the upper thermocline largely determines vertical shear of upper ocean currents in the tropics. This connection to circulation is in part the reason that studies of subsurface temperature variability are needed.

The largest subsurface amplitude is found in the trough near 7.5° N at 100 m. The phase at this latitude tends to increase toward the west, where it terminates in the Mindanao eddy (fig. 6). The phase difference computes to a westward speed of the annual cycle at approximately 25 cm/s. Westward propagation of the annual cycle with similar speed in the central and eastern Pacific in this same latitude band has been noted by Meyers (1979). North of 15° N this westward propagation appears to be absent.

A minimum in amplitude at 100 m running zonally at approximately 20° N (fig. 5) separates the tropical and subtropical regions. The sub-

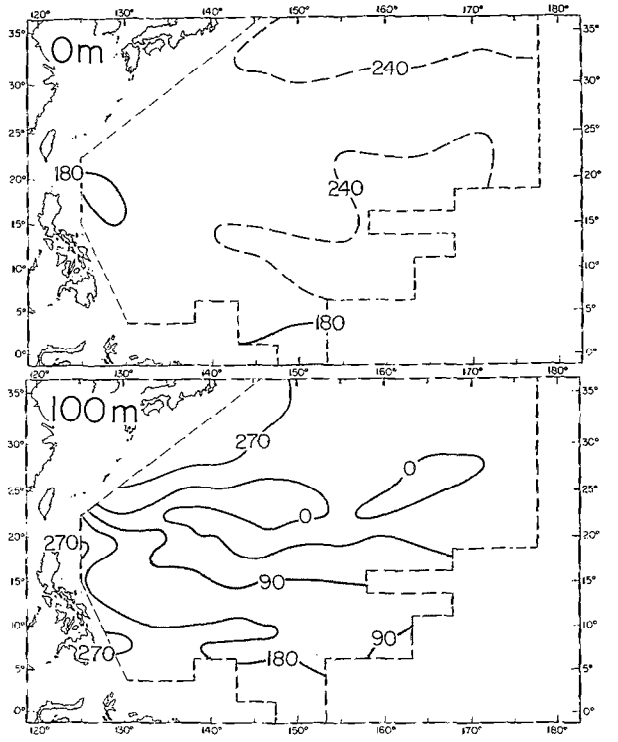

Fig. 6. — Annual phase of temperature variation.
Phase annuelle de la variation de température.

tropical gyre is split in the vicinity of 20° N into subgyres associated with the North Equatorial Current and Subtropical Countercurrent in the south, and the Kuroshio and Kuroshio Countercurrent in the north (HASUNUMA and YOSHIDA, 1978). The center of the southern subgyre appears on the mean temperature map for 100 m (fig. 3) as a warm pool near 15° N, with water exceeding 26° C. The northern subgyre was not well resolved by the 5° longitude gridding used in this study because the Kuroshio and its Countercurrent are very narrow. Its center appears only in the deflection of the 19 °C isotherm south of Japan. The minimum in amplitude at 20° N separates the two subgyres. The annual cycle of the northern subgyre is dominated by temperature change in the surface waters associated with the changing heat flux through the sea surface. The map of annual phase (fig. 6) shows that the upper 100 m is warmest in September (240°-270°). The annual cycle of the southern subgyre is located in the main thermocline, and is not associated with the surface heat flux. The phase there leads the phase of the northern gyre by 3-6 months (90°-180°). The amplitude minimum appears at subsurface levels but not at the surface because upper ocean currents in the two gyres are related to horizontal temperature gradients in the main thermocline.

The zonal alignment of features on the horizontal maps suggests that averaging over a longitudinal band wider than 5° is appropriate, except near the western boundary. Greater stability of monthly means estimated from a larger sample was needed in order to achieve meaningful error limits for estimated amplitude and phase. Also, horizontal maps of the semiannual amplitude and phase (not presented) had significant variations only at the surface and near the trough at 7.5° N (100 m) ; but otherwise, were dominated by noise. The monthly mean temperatures were therefore calculated again in a 15° longitudinal band, near 150° E, where the sampling density (fig. 1) is best.

4. VERTICAL TEMPERATURE FIELD

The meridional section of mean temperature in the band 142.5°-157.5° E and its associated RMS deviation again show the contrast between surface variability in the subtropics north of 20° N and subsurface variability in the main thermocline in the tropics south of 15° N (fig. 7). A minimum of RMS deviation is located between the two regions.

Decomposition of the variance into annual and semiannual components shows that the annual amplitude (fig. 8) is dominant in the subtropical surface layer north of 20° N, the semiannual

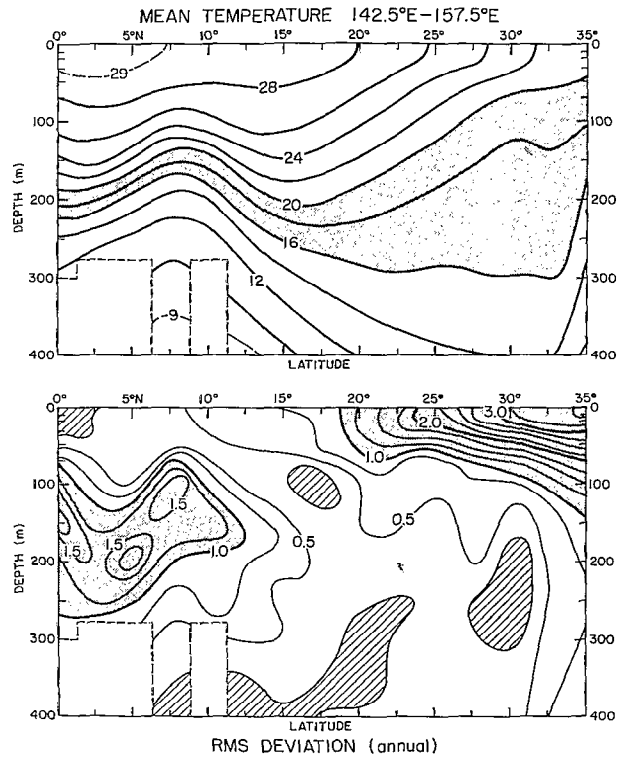

Fig. 7. -- Annual longterm mean temperature and RMS deviation of monthly mean temperatures near 150° E.;

Température annuelle moyenne sur une longue période et écart quadratique moyen de la température mensuelle moyenne au voisinage de 150° E.

amplitude (fig. 9) being smaller by nearly an order of magnitude. The annual amplitude (fig. 8) is large in the North Equatorial Current (7.5° N-15° N), while the semiannual amplitude (fig. 9) is large in the Countercurrent (2.5° N-7.5° N).

The annual phase (fig. 8) shows a contrast between variations at the surface and in the main thermocline. North of 15° N there is a vertical gradient in phase at 100 m-150 m depth. Downward propagation of the annual heating wave (SVERDRUP *et al.*, 1942, p. 135) from the surface to 200 m is indicated by the increasing phase with depth north of 30° N. Phase within the depth range of the main thermocline south of 20° N is nearly vertically uniform, indicating change in depth of the thermocline, with little change in the vertical temperature gradient. This variability suggests a low vertical mode baroclinic response to atmospheric forcing (LIGHTHILL, 1969). Phase in the Countercurrent (5° N) decreases with depth (i.e. phase velocity is upward); however, this is in a region where the amplitude is very small. There is a sharp vertical gradient in phase at 100 m near 15° N. The rapid change in

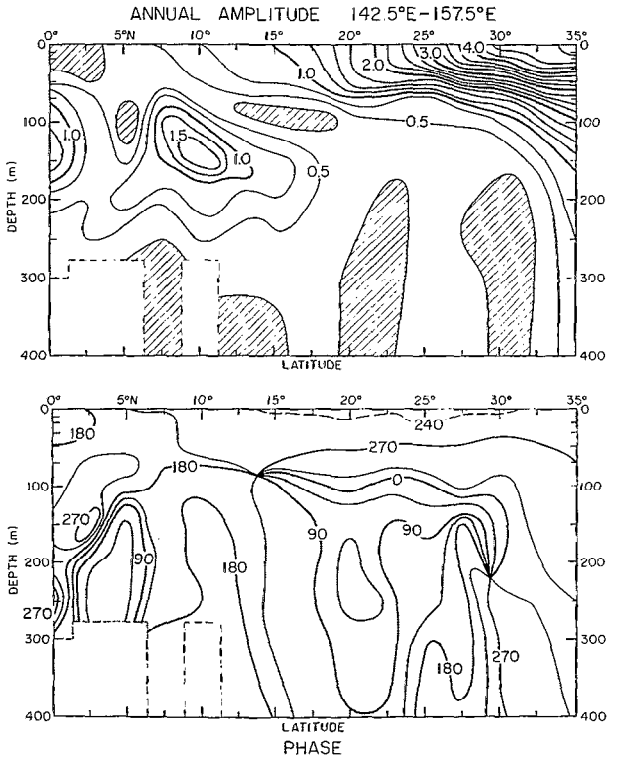

Fig. 8. — Annual amplitude (unit : °C) and phase (unit : ° of angle) near 150° E.

Amplitude (unité : °C) et phase (unité: ° d'angle) annuelles au voisinage de 150° E.

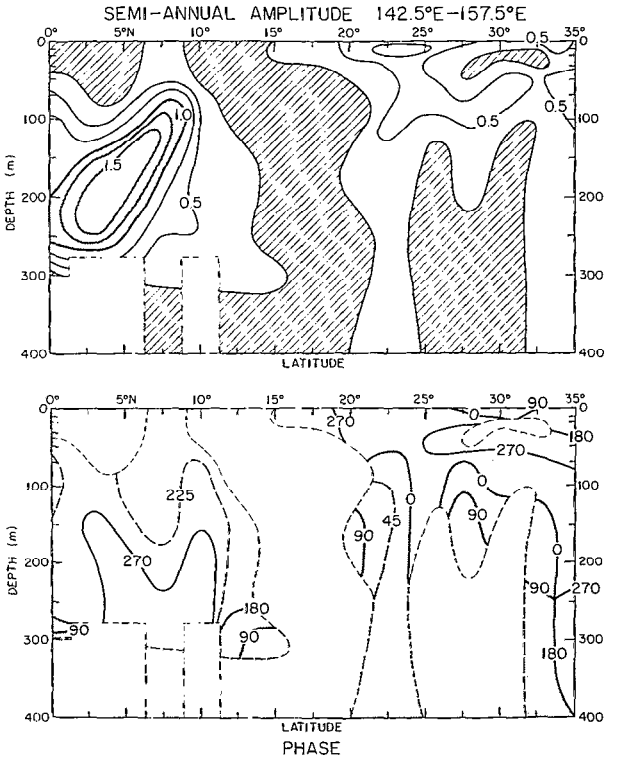

Fig. 9. — Semi-annual amplitude and phase (same units as Fig. 8) near 150° E. Phase is not contoured in the region where amplitude < 0,25 °C.

Amplitude et phase de la composante semi-annuelle (mêmes unités que sur la fig. 8); la phase n'est pas figurée là où l'amplitude est < 0,25 °C.

phase occurs at a level which separates the shallow region dominated by the surface thermohaline process and the deeper baroclinic response in the main thermocline. Amplitude at the maximum phase gradient is very small because the two processes are nearly destructively superimposed at this level. During analysis of the phase, amphidromic points were introduced in this region at locations where the amplitude is very small (<.25 °C), because the phase is indeterminate.

The semiannual phase (fig. 9, bottom) could not be contoured with suitably large spatial scales in the areas where amplitude is less than .25 °C. A large area in the tropical thermocline within the Countercurrent has nearly uniform phase of 225°-270°.

5. DYNAMIC HEIGHT

Dynamic height (0/200 db) was calculated from the monthly mean temperatures, averaged in the band 142.5° E-157.5° E, assuming a uniform value of 34.5 0/00 for salinity. This estimate of dynamic height shows the influence of the vertical integral of temperature on baroclinic structure. This integral

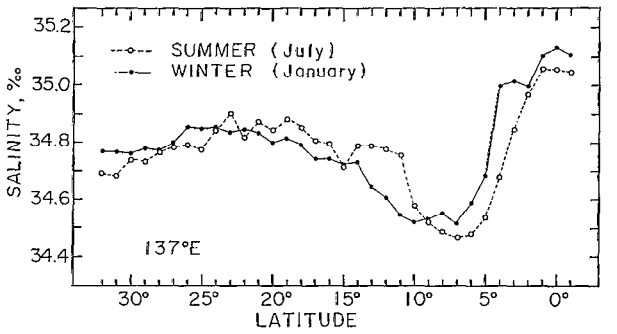

Fig. 10. — Mean January and July salinity along 137° E, averaged 9/200 m. Data from R/V Ryofu Maru cruises 1972-1975.

Salinité de janvier à juillet: moyennes calculées sur les 200 premiers mètres (données des croisières du R.V. Ryofu Maru de 1972 à 1975).

is the most important factor in temporal variability of dynamic height. Neglecting details of the salinity field (fig. 10) introduces errors which are too small to invalidate the conclusions given below (WHITE

et al., 1978 ; WHITE and HASUNUMA, 1980). The annual mean dynamic height (fig. 11, top) has a series of ridges and troughs at 2.5° N, 7.5° N, and 15° N, which are well known from earlier studies (WHITE and HASUNUMA, 1980). Changing strength of the major surface baroclinic currents is indicated by height differences between these ridges and troughs. Annual RMS deviation in dynamic height (indicated by vertical bars) is largest at the equator, 7.5° N, and 35° N (fig. 10, top). The large variance at 35° N is associated with temperature change in the surface mixed layer and not in the main thermocline (compare fig. 11 and 7). In contrast variance at 7.5° N is largely due to temperature change within the depth range of the main thermocline.

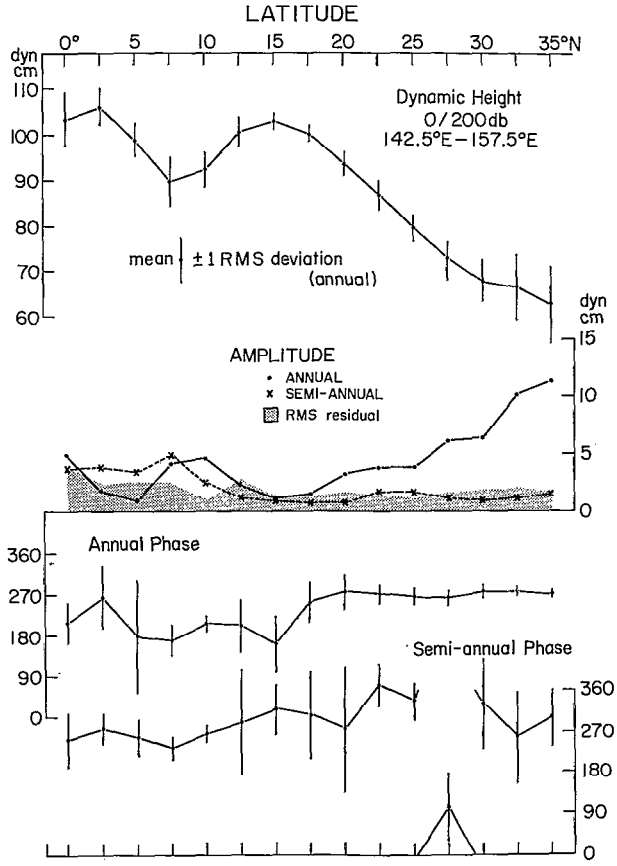

Fig. 11. — Dynamic height 0/200db averaged in 142.5° E to 157.5° E. *Top* : Annual longterm mean and RMS deviation (vertical bars). *Middle* : Annual and semi-annual amplitude. Height of the shaded region indicates RMS residual associated with higher harmonics. *Bottom* : Annual and semi-annual phase, with error limits which are approximately two standard deviations.

Moyennes des hauteurs dynamiques 0/200 db entre 142,5° E et 157,5 E. En haut : *moyenne annuelle sur une longue période et écart quadratique moyen (traits verticaux).* Au milieu : *amplitudes annuelle et semi-annuelle; la hauteur de la partie tramée indique la valeur du résidu de l'écart quadratique moyen lié aux harmoniques de rang élevé.* En bas : *phases annuelle et semi-annuelle, avec indication des limites d'erreur (approximativement deux fois l'écart-type).*

Decomposition of the dynamic height variability into annual and semiannual components (fig. 11, middle) shows that the largest annual amplitude (>10 dyn. cm) occurs in the subtropical region north of 25° N. Secondary maxima are located near the Countercurrent trough at 7.5° N and at the equator. The height of the shaded region indicates the RMS residual variance not accounted for by the annual and semiannual components. The residual (designated δ in section 2) is approximately twice the standard deviation in amplitude. The annual amplitude exceeds the residual nearly everywhere between the equator and 35° N. The semiannual amplitude exceeds the residual and is larger than the annual amplitude between the equator and 10° N.

The annual phase (fig. 11, bottom) changes abruptly from approximately 270° north of 20° N to approximately 180° south of 15° N. The shift occurs because surface variations are dominant in the north, while subsurface variations are dominant in the south (fig. 8, top). Apparently the change in phase owes its existence to the different processes forcing the baroclinic response in the tropics and subtropics. The semiannual phase is nearly uniform in the latitude band, where the amplitude is largest. Error bars approximately equal to twice the standard deviation in phase were estimated as explained in section 2.

The harmonic coefficients presented in fig. 11 were used to construct a smooth estimate of dynamic height at the principal ridges and troughs (fig. 12). The unsmoothed dynamic height data is also shown as well as 90 % confidence limits, estimated from the number of observations and standard deviation (assumed to be uniformly 10 dyn. cm). It is seen that the smooth curves almost always fall within the 90 % confidence limits of the observed points, indicating that the first two harmonics account for much of the known annual cycle in dynamic height.

The difference in dynamic height across the major currents (Subtropical Countercurrent, North Equatorial Current and North Equatorial Countercurrent) was calculated from the harmonic coefficients as well as individual monthly data (fig. 13). The annual cycle in the North Equatorial Current and Countercurrent has a distinct 2 cpy component associated with temperature change within the depth range of the thermocline. This response is probably wind driven. The strength of the Subtropical Countercurrent is dominated by annual heating and cooling on its northern side. Thus, it appears that the tropical and subtropical baroclinic

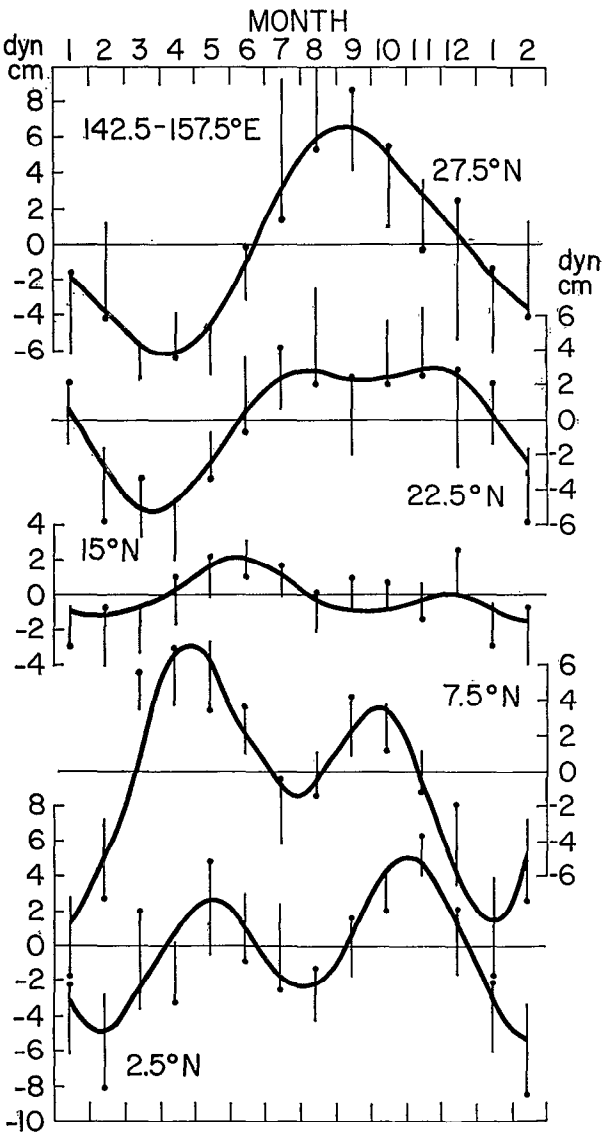

Fig. 12. — Dynamic height 0/200db at the Equatorial Ridge (2.5° N), Countercurrent Trough (7.5° N), North Equatorial Ridge (15° N) and Subtropical Trough (27.5° N). Confidence limits (90 %) are indicated by vertical bars drawn on one side of the data points.

Hauteur dynamique 0/200 db au niveau de la crête équatoriale (2,5° N), du creux du contre-courant (7,5° N), de la crête nord-équatoriale (15° N) et du creux subtropical (27,5 N); l'intervalle de confiance (à 90 %) est figuré par un trait vertical issu du point représentatif.

currents of the western Pacific respond to both wind and thermohaline atmospheric forcing. Their annual cycle is rich in spatial structure and has at least two significant time scales (1 year and 6 months). Developing a dynamical model of this complex system should be a challenging task for future studies.

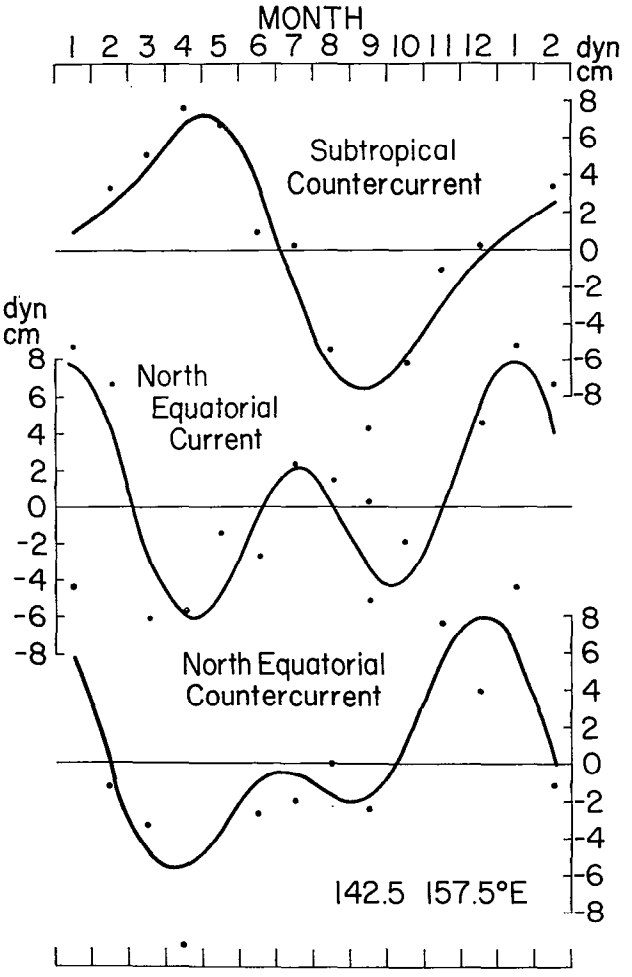

Fig. 13. — Strength of the major baroclinic surface currents, indicated by the dynamic height 0/200db difference between the ridge and through on either side. Monthly differences (dots) and smooth values (solid curves) were estimated from the date in fig. 11.

Intensité des principaux courants baroclines de surface, indiquée par la différence de hauteur dynamique entre la crête et le creux situés de part et d'autre; les différences mensuelles (points) et les valeurs lissées (courbes) ont été déterminées à partir des valeurs de la fig. 11.

6. CONCLUSION

In addition to the annual variation in baroclinic structure, there exists interannual variability, observed both in sea level (WYRTKI, 1975, 1977, 1979) and subsurface temperature (MASUZAWA and NAGASAKA, 1975; WHITE and HASUNUMA, 1980, called WH below). The purpose of this discussion is to compare the spatial structure of variability at these two time scales.

The largest subsurface temperature variance for both annual and interannual scales is found within

the depth range of the main thermocline in the tropics south of 20° N (fig. 7 ; WH fig. 14). Minimum temperature variance in both cases is located between 20° N and 30° N in the Subtropical Mode Water. Annual variation in temperature at higher latitude occurs principally in the upper 100 m; not so interannual variation, where maximum variance occurs in the depth range of the main thermocline beneath the Kuroshio.

The largest annual variations are aligned along the mean ridges and troughs of the temperature field, and show substantial phase differences between currents (fig. 8). The interannual variations are more uniform in phase throughout the tropics from the equator to 20° N (WH, fig. 5, top). Interannual variations are largest in the vicinity of the North Equatorial Countercurrent between the equator and 10° N and in the depth range of the thermocline. Curiously, the annual variation is located in the same region. This suggests that a modulation or interruption of the atmospheric processes that maintain the annual or semiannual variation could play a role in forcing the interannual variation. This hypothesis will be tested in a future study, using long time series of monthly indices of baroclinic structure.

ACKNOWLEDGEMENTS

This research has been supported by the U.S. National Science Foundation under the North Pacific Experiment of the International Decade of Ocean Exploration ; this support is gratefully acknowledged.

Manuscrit reçu au Service des Éditions de l'O.R.S.T.O.M. le 30 septembre 1981.

REFERENCES

BERNSTEIN (R. L.) and WHITE (W. B.), 1977. — Zonal variability in the distribution of eddy energy in the mid-latitude North Pacific. *J. Phys. Oceanogr.*, 7(1) : 123-126.

BLOOMFIELD (P.), 1976. — Fourier Analysis of Time Series An Introduction. John Wiley and Sons, New York, 258 p.

BUSALACCHI (A. J.) and O'BRIEN (J. J.), 1980. — The seasonal variability in a model of the tropical Pacific. *J. Phys. Oceanogr.*, 10(12) : 1929-1951.

COX (M. D.), 1980. — Generation and propagation of 30-day waves in a numerical model of the Pacific. *J. Phys. Oceanogr.*, 10(8) : 1168-1186.

HANEY (R. L.), SHIVER (W. S.) and HUNT (K. H.), 1978. A dynamical-numerical study of the formation and evaluation of large-scale ocean anomalies. *J. Phys. Oceanogr.*, 8(6) : 952-969.

HASUNUMA (K.) and YOSHIDA (K.), 1978. — Splitting of the subtropical gyre in the western North Pacific. *J. Oceanogr. Soc.*, Japan 34(4)(: 170-172.

HUANG (J. C.), 1979. — Numerical simulation studies for oceanic anomalies in the North Pacific basin : II. Seasonally varying motions and structures. *J. Phys. Oceanogr.*, 9(1) : 37-56.

JODC. — Japan Oceanographic Data Center, 1975. Marine Environmental Atlas Northwestern Pacific Ocean. *Japan Hydrographic Association*, Tokyo, 164 pp.

LE ROY (R. D.), 1979. — Tropical disturbances in an oceanic general circulation model with seasonal forcing. MS Thesis, *Naval Postgraduate School*, Monterey, California, 67 pp.

LIGHTHILL (M. J.), 1969. — Dynamic response of the Indian Ocean to the onset of the southwest monsoon. *Phil. Trans. Roy. Soc. London A*, 265 (1159) : 45-92.

MASUZAWA (J.) and NAGASAKA (K.), 1975. — The 137° E oceanographic section. *J. Marine Res.*, 33 (Suppl.) : 109-116.

MEYERS (G.) and DONGUY (J. R.), 1980. — An XBT network with merchant ships. Unpublished manuscript. *Tropical Ocean-Atmosphere Newsletter 2*, 6-7 (Ed. D. Halpern, NOAA Pacific Marine Environmental Laboratory, 3711 15th Avenue NE, Seattle, Washington 98105).

MEYERS (G.), 1975. — Seasonal variation in transport of the Pacific North Equatorial Current relative to the wind field. *J. Phys. Oceanogr.*, 5(3) : 442-449.

MEYERS (G.), 1979. — On the annual Rossby wave in the tropical North Pacific. *J. Phys. Oceanogr.*, 9(4) : 663-674.

RASMUSSON (E. M.) and CARPENTER (T. H.), 1980. — SST lag relationships in the eastern Pacific. *Tropical Ocean-Atmosphere Newsletter 4*, 1-2. (Ed. D. Halpern, NOAA Pacific Marine Environmental Laboratory, 3711 15th Avenue NE, Seattle, Washington 98105).

ROBINSON (M. K.) and BAUER (R. A.), 1976. — Atlas of North Pacific Ocean Monthly Mean Temperatures and Mean Salinities of the Surface Layer. Naval Oceanographic Office, Ref. Publ. 2, Washington, D.C. 19 p., 173 plates.

SVERDRUP (H. U.), JOHNSON (M. W.) and FLEMING (R. H.), 1952. — The Oceans : Their Physics, Chemistry, and General Biology. Prentice-Hall, Englewood Cliffs, 1087 pp.

UDA (M.) and HASUNUMA, 1969. — The eastward Subtropical Countercurrent in the western North Pacific Ocean. *J. Oceanogr. Soc.*, Japan 25(4) : 201-210.

USSR Navy, 1976. — Atlas of the Ocean. : Pacific Ocean., Pergamon Press, New York, 302 pp.

WHITE (W.) and WYLIE (R.), 1977. — Annual and seasonal maps of the residual temperature in the upper waters of the western North Pacific from 1954-1974. SIO Ref. 77-28, *Scripps Inst. of Oceanogr.*, Univ. of Calif., San Diego.

WHITE (W.), HASUNUMA (K.) and SOLOMON (H.), 1978. — Large-scale seasonal and secular variability of the subtropical front in the western North Pacific from 1954-1974. *J. Geophys. Res.*, 83(9) : 4531-4544.

WHITE (W.) and HASUNUMA (K.), 1980. — Large-scale interannual variability in the baroclinic gyre structure of the western North Pacific from 1954-1974. *J. Mar. Res.*, 38(4) : 651-672.

WHITE (W.), MEYERS (G.) and HASUNUMA (K.), 1981. — Space/time statistics of short-term climatic variability in of the western North Pacific. *J. Geophys. Res.* (in review).

WILSON (W. S.) and DUGAN (J. P.), 1978. — Mesoscale thermal variability in the vicinity of the Kuroshio extension. *J. Phys. Oceanogr.*, 8(3) : 537-540.

WYRTKI (K.), 1965. — The annual and semiannual variation of sea surface temperature in the North Pacific Ocean. *Limnol Oceanogr.*, 10(3) : 307-313.

WYRTKI (K.), 1974a. — Sea level and the seasonal fluctuations of the equatorial currents in the western Pacific Ocean. *J. Phys. Oceanogr.*, 4(1) : 91-103.

WYRTKI (K.), 1974b. — Equatorial currents in the Pacific 1950-1970 and their relations to the trade winds. *J. Phys. Oceanogr.*, 4(3) : 372-380.

WYRTKI (K.), 1975. — El Nino — The dynamic response of the equatorial Pacific Ocean to atmospheric forcing. *J. Phys. Oceanogr.*, 5(4) : 572-584.

WYRTKI (K.), 1977. — Sea level during the 1972 El Nino. *J. Phys. Oceanogr.*, 7(6) : 779-787.

WYRTKI (K.), 1979. — The response of sea surface topography to the 1976 El Nino *J. Phys. Oceanogr.*, 9(6) : 1224-1231.

WYRTKI (K.) and LESLIE (W. G.), 1980. — The mean annual variation of sea level in the Pacific Ocean. Hawaii Institute of Geophysics Technical Report HIG-80-5, University of Hawaii, 159 p.